

# Temperature Dependence of the Piezotronic Effect in ZnO Nanowires

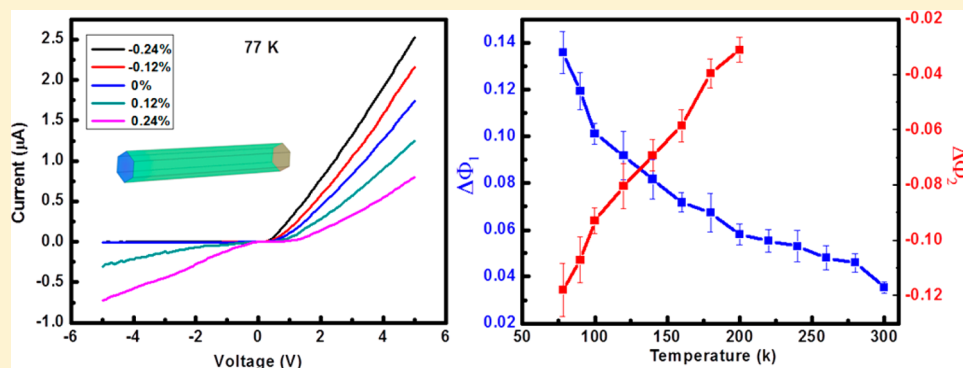
Youfan Hu,<sup>†</sup> Benjamin D. B. Klein,<sup>‡</sup> Yuanjie Su,<sup>†</sup> Simiao Niu,<sup>†</sup> Ying Liu,<sup>†</sup> and Zhong Lin Wang<sup>\*,†,§</sup>

<sup>†</sup>School of Material Science and Engineering, Georgia Institute of Technology, Atlanta, Georgia 30332-0245, United States

<sup>‡</sup>School of Electrical and Computer Engineering, Georgia Institute of Technology, Atlanta, Georgia 30332-0250, United States

<sup>§</sup>Beijing Institute of Nanoenergy and Nanosystems, Chinese Academy of Sciences, Beijing 100190, China

**S** Supporting Information



**ABSTRACT:** A comprehensive investigation was carried out on n-type ZnO nanowires for studying the temperature dependence of the piezotronic effect from 77 to 300 K. In general, lowering the temperature results in a largely enhanced piezotronic effect. The experimental results show that the behaviors can be divided into three groups depending on the carrier doping level or conductivity of the ZnO nanowires. For nanowires with a low carrier density ( $<10^{17}/\text{cm}^3$  at 77 K), the piezotronic effect is dominant at low temperature for dictating the transport properties of the nanowires; an opposite change of Schottky barrier heights at the two contacts as a function of temperature at a fixed strain was observed for the first time. At a moderate doping (between  $10^{17}/\text{cm}^3$  and  $10^{18}/\text{cm}^3$  at 77 K), the piezotronic effect is only dominant at one contact, because the screening effect of the carriers to the positive piezoelectric polarization charges at the other end (for n-type semiconductors). For nanowires with a high density of carriers ( $>10^{18}/\text{cm}^3$  at 77 K), the piezotronic effect almost vanishes. This study not only proves the proposed fundamental mechanism of piezotronic effect, but also provides guidance for fabricating piezotronic devices.

**KEYWORDS:** piezotronic effect, ZnO, nanowire

For wurtzite structured materials, such as ZnO, GaN, and InN, due to the noncentral symmetry, a piezoelectric potential (piezopotential) is created in the crystal under strain. Owing to the coupling of semiconducting and piezoelectric properties, the piezotronic effect involves using the strain-induced inner-crystal piezopotential as a “gate” to tune/control the charge carrier transport properties of a p–n junction or metal–semiconductor interface. This new concept was first proposed in 2007.<sup>1,2</sup> A series of electronic devices have been demonstrated based on this effect, including piezopotential gated field-effect transistors,<sup>3</sup> piezopotential gated diodes,<sup>4</sup> strain sensors,<sup>5</sup> force/flow sensors,<sup>6</sup> hybrid field-effect transistors,<sup>7</sup> piezotronic logic gates,<sup>8</sup> electromechanical memories,<sup>9</sup> and so forth. Great potential for the application of this new effect and research field has been demonstrated. As of now, all of the experimental studies were carried out at room temperature, and there has been no investigation of temperature effects on the performance of piezotronic devices. Considering the complicated and variable working environment

the devices may experience, the temperature behavior of the piezotronic device is of great significance not only for fully understanding this coupling effect between mechanical and electrical properties in nanomaterials, but also for developing new novel piezotronic devices.

In this work, ultra long ZnO nanowires were placed on flexible substrates with good thermal conductivity. Silver was chosen for the metal electrodes to form Schottky barriers at the two ends of the nanowire. Over 40 devices were characterized for the piezotronic response in a temperature range of 77–300 K. The behaviors can be clearly divided into three groups, which correspond to nanowires with high, moderate, and low carrier densities, respectively. In general, the piezotronic response is largely enhanced with the decrease of temperature. This is attributed to the weakened screening effect from the

Received: May 9, 2013

Revised: August 29, 2013

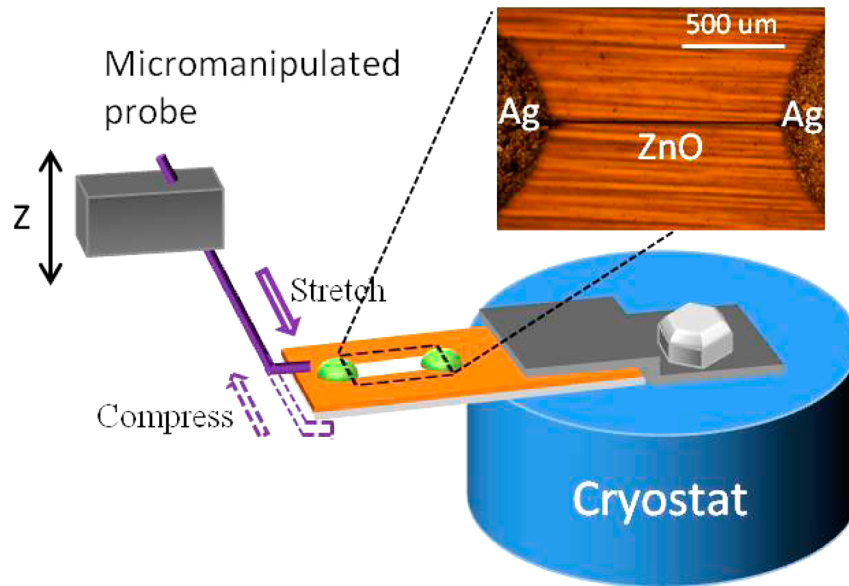


**Figure 1.** Schematic diagram of the experimental setup. A device is fixed on the edge of the cryostat. A micromanipulated probe is used to deform the substrate. The upper right insert is an optical image of a real device.

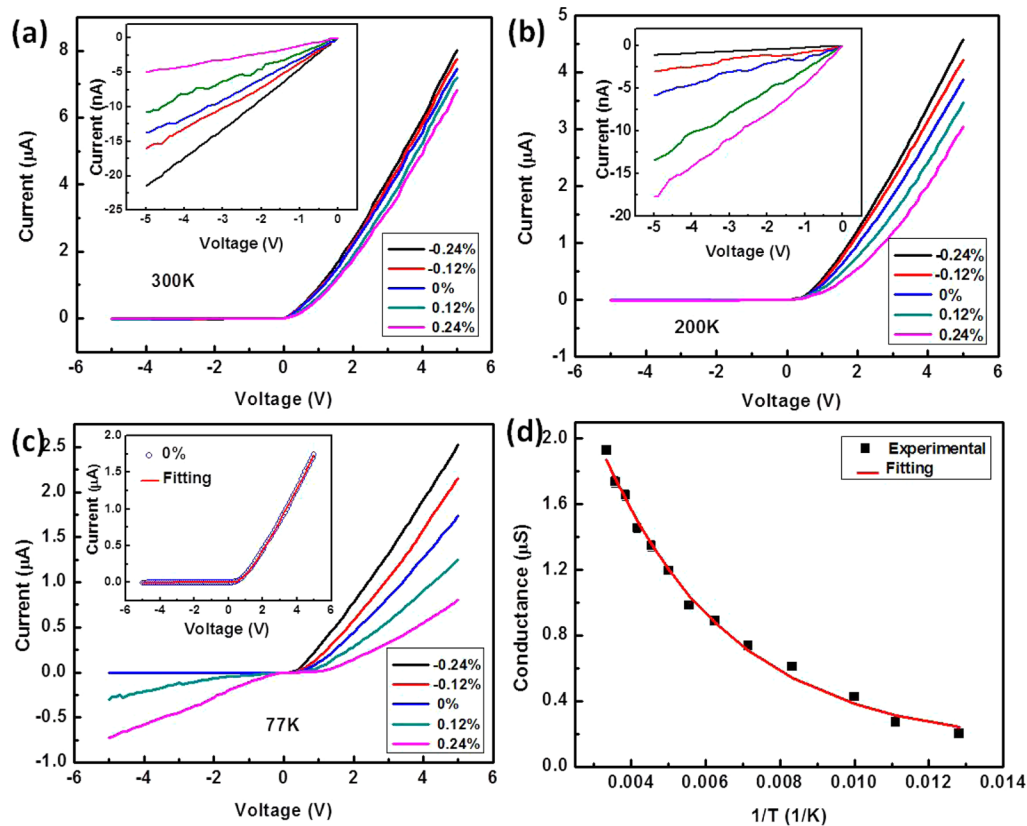


**Figure 2.** Typical temperature dependence behavior of devices with low conductivity. Transport characteristics changes under applied strain at (a) 300 K, (b) 200 K, and (c) 77 K. The inserts of a and b are the enlarged images in negative voltage range. The insert of c is the fitting result of the curve at strain = 0% by using the MSM model. (d) Conductance of the nanowire excluding contacts changing with temperature under no strain. The red line is the fitting curve of the data by using eq 1.

decreased carrier density. An opposite change of Schottky barrier heights at the two contacts as a function of temperature at a fixed strain was observed for the first time in nanowires with low carrier density due to the dominant role of the piezotronic effect at low temperature.

The ultralong ZnO nanowires used in this work were grown by a high-temperature thermal evaporation process.<sup>10</sup> The typical diameter was around 300–600 nm, and the length was several hundred micrometers to several millimeters. The piezotronic assembly and characterization were carried out in a micro manipulation cryogenic probe system (Janis, model ST-

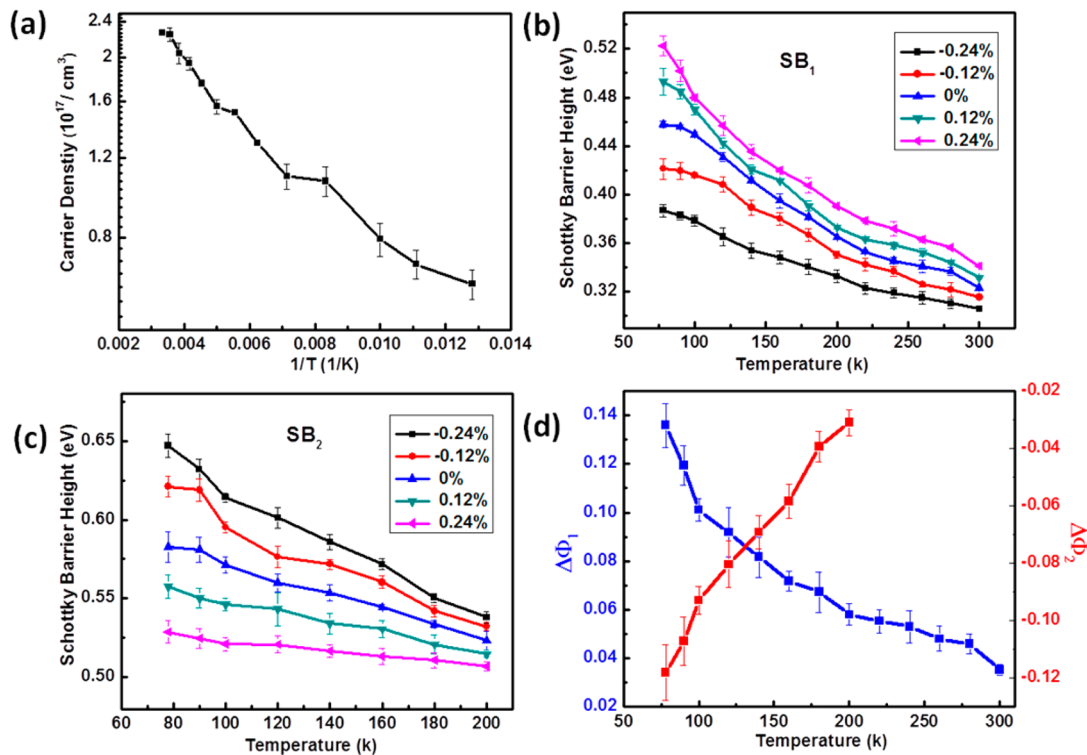


**Figure 3.** (a) Carrier density change as a function of inverse temperature for nanowires with low conductivity. (b and c) Change of relevant Schottky barrier heights at the two contact areas with applied strain and temperature. (d) Temperature dependence of barrier height change  $\Delta\Phi_{0.24\%} - \Phi_{-0.24\%}$ . The error bars represent the standard error of the determined parameters.

500-2). The experimental setup is sketched in Figure 1. Working with liquid nitrogen, the system can provide a working environment in the temperature range from 77 to 300 K. To maintain good thermal equilibrium between the nanowires and cryostat, aluminum foil covered with a layer of Kapton tape (both are  $25.4 \mu\text{m}$  in thickness) served as the substrate, which can provide excellent thermal conductivity with an insulating surface and very good mechanical flexibility. The thermal expansion coefficients of aluminum and Kapton tape are similar,  $23.1 \times 10^{-6}/^\circ\text{C}$  and  $20 \times 10^{-6}/^\circ\text{C}$ , respectively. Substrate deformation due to the thermal expansion coefficient mismatch can be neglected. Ultra long ZnO nanowires were picked up and placed on the substrate. Silver pastes were used to create the electrical contacts at the two ends of the nanowire, which formed a metal–semiconductor–metal (M–S–M) structure. As shown in Figure 1, the device was put on the edge of the cryostat, and a micromanipulating probe was used to deform the substrate introducing stretch or compress strain in the nanowires. The upper right insert in Figure 1 is an optical image captured from an actual device. Electrical characterization of the device was carried out under different strain conditions in the temperature range of 77–300 K. The strain in the nanowire is estimated by using the same method as in previous strain sensor work.<sup>5</sup> Quantitative analysis of the experimental data was performed by using a MSM model<sup>11,12</sup> to obtain the relevant device parameters, including conductance of the nanowire excluding contacts, carrier density, Schottky barrier height, and so forth. The behavior of piezotronic response can be divided into three groups, which corresponding to different conductivity in ZnO nanowires.

Figure 2a–c shows the piezotronic response characteristics of the first group of devices. For these devices, the changes of  $I$ – $V$  curves under applied strain were observed at 300 K. The

current increased or decreased simultaneously in both the positive and the negative voltage range but with different magnitudes. The changes of the  $I$ – $V$  curves were nonsymmetrical. As the temperature decreased further, the change of  $I$ – $V$  curves became more significant under strain. Starting from 200 K, the changes of the current in the positive and negative voltage ranges exhibited opposite signs. When the temperature reached 77 K, this trend became very pronounced. This is the first time that we observed such a phenomenon. To elaborate the physical mechanism here, we extracted the related device parameters by simulating the electrical transport properties quantitatively through a MSM model.<sup>11,12</sup> In this model, the M–S–M structure is simulated as two Schottky barriers connected back to back through a resistor, which represent two metal–semiconductor contacts and the semiconducting nanowire, respectively. The key assumptions of this model include that, first, the length of the nanowire between two electrodes is longer than the carrier’s mean free path. So the transport lies within the diffusive regime and Ohmic law can be used to describe the conductance of carriers in the undepleted part of the nanowire. Generally, for our devices, the length of nanowire between two electrodes is around 1 mm, which is far beyond the electron mean free path of ZnO nanowires. Second, this model is valid when the radius of the nanowire is larger than the electron de Broglie wavelength. In such condition, electron–electron and electron–phonon interaction can be ignored, and the effective mass approximation is valid. Third, the doping is uniform in the nanowire, and the contact areas at the two electrodes are equal. We use thermionic emission theory to describe the forward biased Schottky barrier’s behavior, while for the reverse-biased one, thermionic field emission or field emission theory is used to describe it depend on working temperature. Considering that the nanowire and

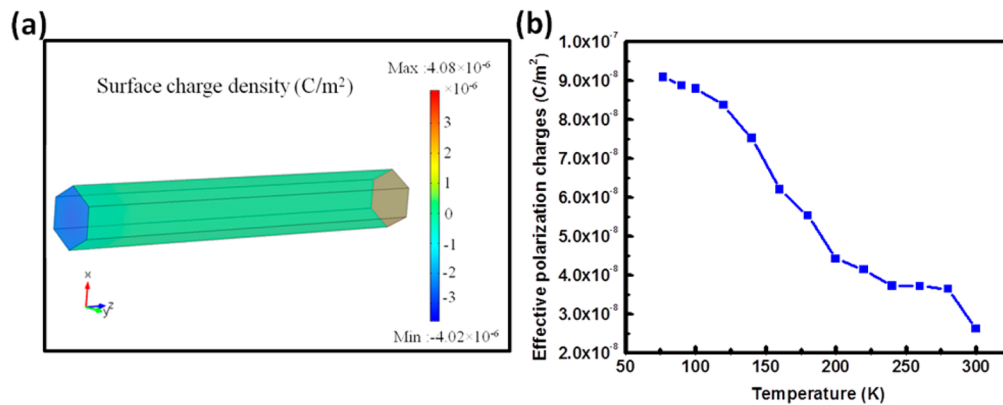


**Figure 4.** (a) FEM simulation result to show polarization charges generate at the two ends of the nanowire with opposite signs. (b) Temperature dependence of effective polarization charges at the nanowire's end surface after considering the screening effect.

two Schottky barriers are serially connected, a current–voltage equation set can be obtained between these three parts. The numerical solution of this equation set is carried out by using Newton method through a well-developed Matlab based program PKUMSM.<sup>12</sup> The obtained parameters include the carrier density, carrier mobility, conductance of the nanowire excluding contacts, and the effective heights of the two Schottky barriers, and so forth. The effective Schottky barrier height here is a physical parameter that is used to describe the overall transport properties through the contact. The insert of Figure 2c is a representing fitting curve. The extracted carrier density change under different strains at the same temperature is smaller than 5%, thus eliminating it as a possible contribution to the observed Schottky barrier changes at the same temperature under different strain condition. As shown in Figure 2d, the obtained conductance of the nanowire excluding contacts decreased as the temperature decreased, which is a typical semiconductor behavior. This is because that the carrier density is supplied by ionization of shallow level dopants. It decreases with decreasing temperature due to freeze-out, leading to a decreased conductance at lower temperature. For thermally activated transport, the conductivity can be approximately expressed as:<sup>13</sup>

$$G(T) = G_0 \exp(-E_D/k_B T) \quad (1)$$

where  $E_D$  is the thermal activation energy of donor states and  $k_B$  is the Boltzmann constant. The fitted thermal active energy  $E_D$  in Figure 2d is 30 meV, which agrees well with the shallow donor energy level.<sup>14,15</sup> Figure 3a shows the carrier density decreased as the temperature decreased, just as we elaborated. It should be noted here that the carrier density is in a relatively low range, which is around  $2.2 \times 10^{17}/\text{cm}^3$  at 300 K, and decreased to  $6 \times 10^{16}/\text{cm}^3$  at 77 K. Figure 3b and c are the relevant effective Schottky barrier (SB) heights at the two contacts, SB<sub>1</sub> and SB<sub>2</sub>, under different strain conditions at different temperature. First, we check the blue curve, which represent the device under no strain. For both Schottky barriers, the heights increased as temperature decreased. This is because that we use a thermionic field emission model to describe the current transport process through the Schottky barrier. As the temperature decreased, the kinetic energy of thermally excited carriers decreased; thus, the barrier is effectively thicker/higher for them to transport through/over. In addition, lowering the temperature could also change the occupation of surface states. These factors are expressed in our

measurement as causes of increased effective Schottky barrier height.

However, we are more interested in the barrier height changes under fixed strain range, which could be a very good evaluation of the magnitude of the piezotronic effect. As shown in Figure 3d, we plot the relationship of barrier height change  $\Delta\Phi_{0.24\%} - \Phi_{-0.24\%}$  under tensile strain 0.24% and compressive strain  $-0.24\%$  as a function of sample temperature. It is clear that, as the temperature decreased, the change of barrier height increased under the same strain range. The height of SB<sub>1</sub> increased more obviously, while the height of SB<sub>2</sub> decreased more notably. Previous studies show that the coefficients of electromechanical coupling of ZnO are almost independent of temperature, and the change of elastic constants of ZnO is less than 0.5% in the temperature range of 77–300 K.<sup>16</sup> Thus, we attribute this enhanced piezotronic effect at low temperatures as predominantly due to the increased effective polarization surface/interface charge density at the two contacts as the screening effect is reduced by the decreased carrier density. Other contributions may come from the change of junction capacitance owing to the altered depletion region profile change at low temperature.

As shown in Figure 4a, we use the finite element method (FEM) to simulate the polarization charge generation. The length of the nanowire is 2  $\mu\text{m}$ , and the side length of hexagonal cross-section is 150 nm. The nanowire is built along its  $c$ -axis and assumed to be insulating at first. A compressive load of 0.35 GPa was applied at one of the end surface to produce a strain of 0.24% in the nanowire. Polarization charges were generated at the two end surfaces with opposite signs. For the transport of electrons, the Schottky barrier height at the end with negative polarization charges will increase, while the one at the other end with positive polarization charges will decrease. This is what we would expect for the piezotronic effect. But in the actual situation, there is always unintentional n-type doping in ZnO nanowires. These free electrons will partially screen the positive polarization charges. Our previous experimental and theoretical works have shown that it will reduce the piezoelectric potential drop along the nanowire and thus the output performance of a piezoelectric nanogenerator.<sup>17,18</sup> For the piezotronic effect, this screening effect will reduce the effective polarization charges at the surface. According to the theoretical model we built for the piezotronic effect at a metal–semiconductor interface, the Schottky barrier height change induced by polarization charges can be expressed as:<sup>19</sup>

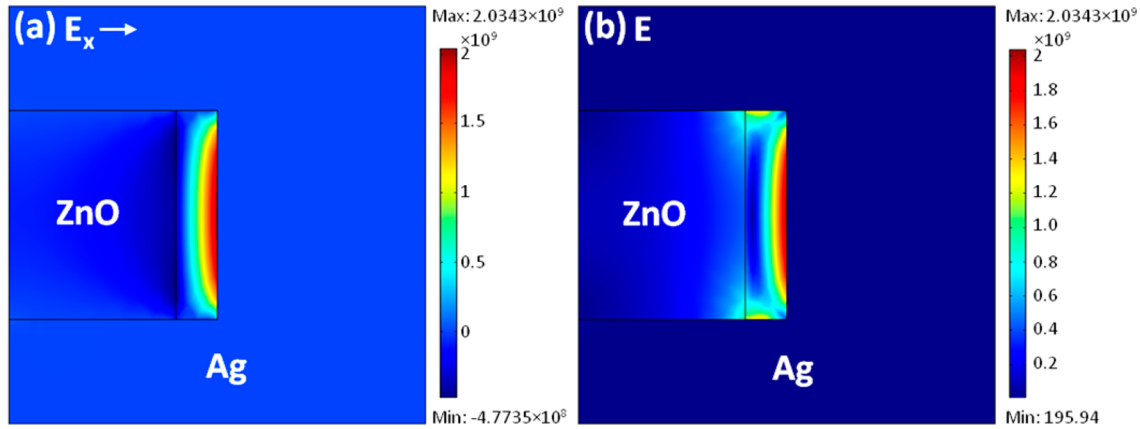


Figure 5. Simulated distribution of electric field around the contact of ZnO nanowire and Ag electrode. (a) Electric field along the axial direction of the nanowire and (b) the magnitude of the total electric field  $E$ . Simulation details are sketched in the Supporting Information.

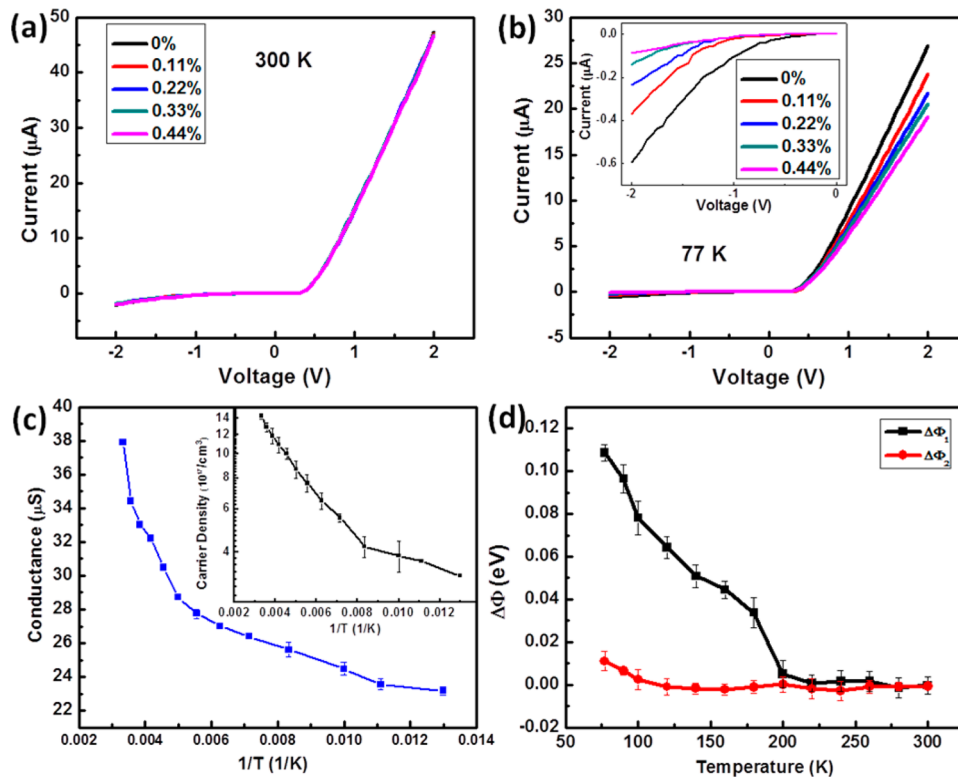
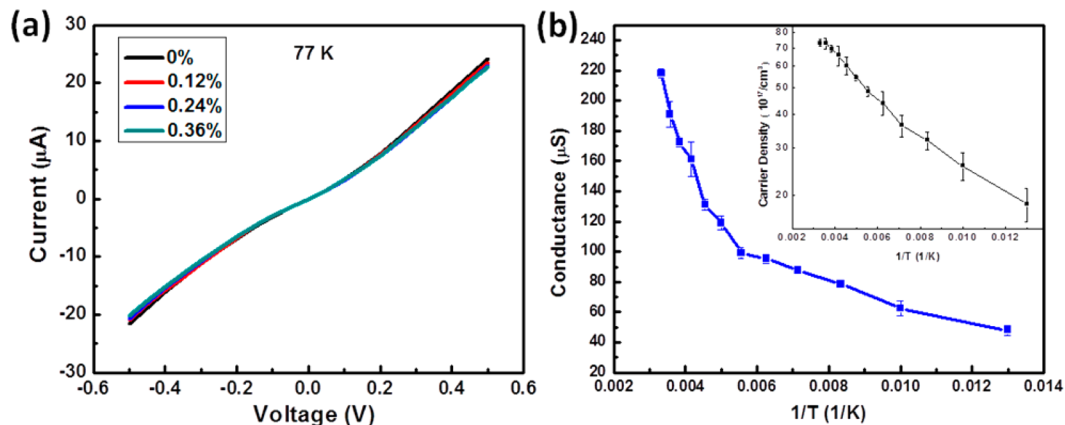


Figure 6. Typical temperature dependence behavior of devices with moderate conductivity nanowires. Transport characteristics changes under applied strain at (a) 300 K and (b) 77 K. (c) Conductance of the nanowire excluding contacts changing with temperature. Inset: Carrier density change with inverse temperature. (d) Schottky barrier height changes at the two contacts with temperature  $\Delta\Phi_{0.44\%} - \Phi_{0\%}$ .

$$\Delta\Phi = -\frac{q^2 \rho_{\text{eff}} W}{2\epsilon_s} \quad (2)$$

in which  $q$  is the absolute value of the unit electronic charge,  $\rho_{\text{eff}}$  is the area density of the effective polarization charges, and  $\epsilon_s$  is the permittivity of ZnO. We assume that the polarization charges distribute at the metal–semiconductor interface within a very thin layer with a width of  $W$ . The change of Schottky barrier height is proportional to the effective polarization charges at the interface area. Positive polarization charges will decrease the barrier height, while negative charges will increase the barrier height. As for an M–S–M structure, the transport property of the device was controlled dominantly by the Schottky barrier under reverse bias. So, we would expect that

the current will change oppositely under positive and negative bias voltages when strain is applied as different Schottky barriers will be dominant in these two situations. But, generally, in our previous results,<sup>5,8,9</sup> we only observed that the absolutely measured current either increased or decreased simultaneously at a nonsymmetrical manner under both bias voltages. This is a result coming from the combination of piezotronic effect and band structure change (e.g., piezoresistance effect). The latter is a symmetrical effect on both Schottky barriers. As temperature decreased, carrier density in the nanowire decreased, and thus the screening effect reduced. So the  $\rho_{\text{eff}}$  increased continuously, and at certain point, the piezotronic effect will take over the band structure change. In such a case, Schottky barrier height increased at one end and decreased at the other end under



**Figure 7.** Typical temperature dependence behavior of devices with high conductivity. (a) Transport characteristics changes under applied strain at 77 K. (b) Conductance of the nanowire excluding contacts changing with temperature. Insert: Carrier density change with inverse temperature.

applied strain. The current will change oppositely under positive and negative bias voltage as we have observed in Figure 2c.

Furthermore, the ZnO nanowire contacts the Ag electrode in two ways: its end surface that have piezoelectric polarization charges due to the *c*-axis orientation of the nanowires, and the side surfaces that may have no piezoelectric charges. We have carried out a numerical simulation about the distribution of electric field in ZnO nanowire surrounded by Ag electrode with and without the presence of piezoelectric charges (see Supporting Information). According to this simulation, most of the electric field is localized near the end polar surface of the nanowire, which is also the area where piezoelectric charges are distributed as shown in Figure 5. The electric field at the end surface and side surface are both increased, while the change of the former one is several orders of magnitudes larger than the latter one. Therefore, the transport property at the ZnO–Ag contact is dominated by the end surface. In addition, although the piezoelectric charges are only located at the end surface of ZnO, they can affect the electrical field distribution in the whole contact area and the overall transport properties through the contact. This is the base of our interpretation why the piezotronic effect dominates the transport in our case.

To reveal how the density of polarization charges are changed with temperature quantitatively, we first evaluate the effective surface charges at the metal–semiconductor interface as below,<sup>20,21</sup>

$$\rho_s = \sqrt{2\epsilon_r\epsilon_0kT \left[ N_D \left( \frac{\Phi}{kT} \right) + n_{\text{bulk}} \left( \exp\left( \frac{-\Phi}{kT} \right) - 1 \right) \right]} \quad (3)$$

where  $\rho_s$  is the total surface charges,  $\Phi$  is Schottky barrier height,  $N_D$  is the donor dopant concentration, and  $n_{\text{bulk}}$  is the temperature-dependent bulk carrier density, which is equal to the ionized donor dopant concentration. Here, we assume that (1) semiconductor is nondegenerate; (2) there are no minority carriers; and (3) the ionized donor dopant concentration is constant everywhere in the semiconductor. The first term in the square brackets represents screening of the surface charges by fixed ionized dopants. The second term is the screening by mobile electrons. If we assume that all of the donor are ionized at room temperature,  $N_D = n_{\text{bulk}}(T=300\text{K})$ . Then, the effective polarization charges  $\rho_{\text{eff}}$  introduced by strain can be expressed as  $\rho_{\text{eff}} = \rho_{s(\text{strain}=-0.24\%)} - \rho_{s(\text{strain}=0\%)}$ . By using the data in Figure 2a and b, the relationship between  $\rho_{\text{eff}}$  and temperature is

plotted in Figure 4b. It shows clear that, as the environment is cooled down, the effective polarization charges increase steadily under the same strain. This contributes to the enhanced piezotronic effect at low temperature.

The behavior of the second group devices is shown in Figure 6. For these devices, there is no response to applied strain at 300 K. As temperature decreased, changes appear in the *I*–*V* curves. As the temperature reached 77 K, when a tensile strain was applied, current decreased simultaneously and nonsymmetrically under both positive and negative bias voltage, as shown in Figure 6b. This means that the piezotronic effect is not as strong as the band structure change effect at that point. Figure 6c is the corresponding conductance and carrier density information of the device obtained from the M–S–M model simulation. The carrier density is around  $1.4 \times 10^{18}/\text{cm}^3$  at 300 K and decreased to  $3 \times 10^{17}/\text{cm}^3$  at 77 K. We can image that the screening effect is still strong at such a high carrier density level at 77 K, which is comparable to the carrier density for Figure 2a at room temperature. A lower temperature may be needed to further decrease the carrier density and make the piezotronic effect dominant, achieving the similar behavior shown in Figure 2c. Figure 6d shows the barrier height changes ( $\Delta\Phi_{0.44\%} - \Phi_{0\%}$ ) at the two contacts with temperature. At a higher temperature range, Schottky barriers were nearly unaffected by applied strain. Then, one of the barriers started to increase at 200 K and elevated quickly as temperature further decreased, while the other one started to increase around 100 K. It indicated that, at first, the piezotronic effect is only dominant at one contact where the negative polarization charges are created. It is consistent with the proposed mechanism of screening effect.

Devices fabricated with very high conductivity nanowires were attributed to the third group. The representative behavior of the piezotronic effect is shown in Figure 7. The typical carrier density of the nanowire is higher than  $1 \times 10^{18}/\text{cm}^3$  at 77 K. The conductance of the nanowire excluding contacts is 2 orders of magnitude larger than the one in the first group. The screening effect is extremely strong in this case. Even at 77 K, there is no obvious response of the electrical transport properties to the applied strain. This means that both the piezotronic effect and the band structure changes are very weak in this case. These highly doped nanowires are not suitable for fabricating piezotronic devices. The fluctuation of conductivity in nanowires is unavoidable during the synthesis process. But a postgrowth treatment can be introduced to narrow the

distribution range and suppress the conductivity, such as treatment with oxygen plasma, annealing in oxygen, and passivating the nanowire surface with certain polymers.<sup>22</sup> Finally, in Figure 8, the carrier density distribution of all

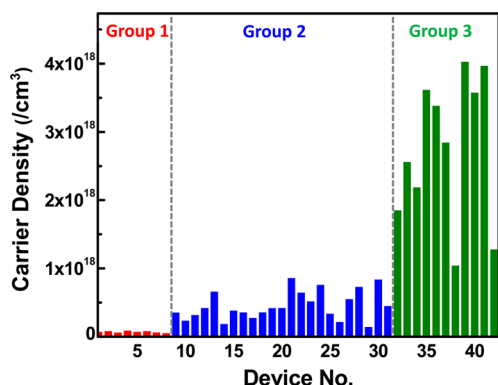


Figure 8. Carrier density distribution of all of the devices measured.

devices under test is plotted. The carrier density range belong to different groups is revealed clearly. The fluctuation of carrier density is obvious, which is normal for nanomaterials.

In conclusion, the temperature dependence of piezotronic effect in ZnO nanowires has been investigated in the temperature range of 77–300 K. After over 40 devices having been tested, the typical behavior can be divided into three groups, corresponding to different carrier density ranges. First of all, piezotronic effect will be enhanced as temperature decreases. We attribute this to the suppressed screening effect from the free carriers at lower temperature due to decreased carrier density in the nanowire. It is the first time that we observed the opposite change of Schottky barrier heights at the two contacts as a function of temperature at a fixed strain. It is a direct proof of the piezo-induced polarization charges at the two ends of the nanowire and the proposed fundamental mechanism of the piezotronic effect.

## ■ ASSOCIATED CONTENT

### 📄 Supporting Information

Model explanation and figures showing the piezoelectric charge distribution. This material is available free of charge via the Internet at <http://pubs.acs.org>.

## ■ AUTHOR INFORMATION

### Corresponding Author

\*E-mail: [zlwang@gatech.edu](mailto:zlwang@gatech.edu).

### Notes

The authors declare no competing financial interest.

## ■ ACKNOWLEDGMENTS

Research was supported by U.S. Department of Energy, Office of Basic Energy Sciences (Award DE-FG02-07ER46394), NSF (0946418), and the Knowledge Innovation Program of the Chinese Academy of Science (Grant No. KJCX2-YW-M13). Patents have been filed based on the research results presented in this manuscript.

## ■ REFERENCES

- (1) Wang, Z. L. *Mater. Today* **2007**, *10* (5), 20–28.
- (2) Wang, Z. L. *Adv. Mater.* **2007**, *19* (6), 889–892.

(3) Wang, X. D.; Zhou, J.; Song, J. H.; Liu, J.; Xu, N. S.; Wang, Z. L. *Nano Lett.* **2006**, *6* (12), 2768–2772.

(4) He, J. H.; Hsin, C. L.; Liu, J.; Chen, L. J.; Wang, Z. L. *Adv. Mater.* **2007**, *19* (6), 781–784.

(5) Zhou, J.; Gu, Y. D.; Fei, P.; Mai, W. J.; Gao, Y. F.; Yang, R. S.; Bao, G.; Wang, Z. L. *Nano Lett.* **2008**, *8* (9), 3035–3040.

(6) Fei, P.; Yeh, P. H.; Zhou, J.; Xu, S.; Gao, Y. F.; Song, J. H.; Gu, Y. D.; Huang, Y. Y.; Wang, Z. L. *Nano Lett.* **2009**, *9* (10), 3435–3439.

(7) Liu, W. H.; Lee, M.; Ding, L.; Liu, J.; Wang, Z. L. *Nano Lett.* **2010**, *10* (8), 3084–3089.

(8) Wu, W. Z.; Wei, Y. G.; Wang, Z. L. *Adv. Mater.* **2010**, *22* (42), 4711–4715.

(9) Wu, W. Z.; Wang, Z. L. *Nano Lett.* **2011**, *11* (7), 2779–2785.

(10) Pan, Z. W.; Dai, Z. R.; Wang, Z. L. *Science* **2001**, *291* (5510), 1947–1949.

(11) Zhang, Z. Y.; Yao, K.; Liu, Y.; Jin, C. H.; Liang, X. L.; Chen, Q.; Peng, L. M. *Adv. Funct. Mater.* **2007**, *17* (14), 2478–2489.

(12) Liu, Y.; Zhang, Z. Y.; Hu, Y. F.; Jin, C. H.; Peng, L. M. *J. Nanosci. Nanotechnol.* **2008**, *8* (1), 252–258.

(13) Sze, S. M. *Physics of semiconductor devices*, 2nd ed.; Wiley: New York, 1981; p xii.

(14) Look, D. C.; Hemsley, J. W.; Szelove, J. R. *Phys. Rev. Lett.* **1999**, *82* (12), 2552–2555.

(15) Reynolds, D. C.; Look, D. C.; Jogai, B. *J. Appl. Phys.* **2001**, *89* (11), 6189–6191.

(16) Kobiakov, I. B. *Solid State Commun.* **1980**, *35* (3), 305–310.

(17) Liu, J.; Fei, P.; Song, J. H.; Wang, X. D.; Lao, C. S.; Tummala, R.; Wang, Z. L. *Nano Lett.* **2008**, *8* (1), 328–332.

(18) Gao, Y.; Wang, Z. L. *Nano Lett.* **2009**, *9* (3), 1103–1110.

(19) Zhang, Y.; Liu, Y.; Wang, Z. L. *Adv. Mater.* **2011**, *23* (27), 3004–3013.

(20) Mönch, W. *Semiconductor Surface and Interfaces*; Springer: Berlin, 1993; p 51.

(21) Chevtchenko, S.; Ni, X.; Fan, Q.; Baski, A. A.; Morkoc, H. *Appl. Phys. Lett.* **2006**, *88* (12), 122104.

(22) Hu, Y. F.; Lin, L.; Zhang, Y.; Wang, Z. L. *Adv. Mater.* **2012**, *24* (1), 110–114.